Angular momentum mixing dynamics of attractive Bose–Einstein condensates on a deformed ring

2009 J. Phys. A: Math. Theor. 42 075305

(http://iopscience.iop.org/1751-8121/42/7/075305)

IOP PUBLISHING JOURNAL OF PHYSICS A: MATHEMATICAL AND THEORETICAL

J. Phys. A: Math. Theor. **42** (2009) 075305 (11pp) doi:10.1088/1751-8113/42/7/075305

Angular momentum mixing dynamics of attractive Bose–Einstein condensates on a deformed ring

Zhifeng Chen and Zhibing Li

State Key Laboratory of Optoelectronic Materials and Technologies, School of Physics and Engineering, Sun Yat-Sen University, Guangzhou, 510275, People's Republic of China

E-mail: stslzb@mail.sysu.edu.cn

Received 11 April 2008, in final form 1 December 2008
Published 21 January 2009
Online at stacks.iop.org/JPhysA/42/075305

Abstract

The Hamiltonian of an attractive N-boson system confined on a ring is diagonalized. The particles have strong correlation as a result of a quantum phase transition in the strong-interaction phase, where the yrast states are quasi-degenerate. It is found that a small deformation of the ring will mix the quasi-degenerate yrast states to form cluster states which break the spatial symmetry explicitly. The time evolution of the average angular momentum in an elliptic ring exhibits strong oscillation.

PACS number: 03.75.Hh

1. Introduction

The Bose–Einstein condensation in low dimension has been realized experimentally [1]. With the use of the Feschbach resonance [2], the formation of matter-wave bright solitons has also been achieved in experiments [3, 4]. These experimental achievements have stimulated intensive theoretical studies on atoms confined in quasi-one-dimensional traps [5–13]. In [5, 6], the one-dimensional Gross–Pitaevskii equation (GPE) in both cases of repulsive and attractive interaction was solved analytically. For the attractive interaction, based on the solutions of [6], a quantum phase transition that breaks the translational symmetry is proposed under the mean-field theory (MFT) [7, 8]. In [9], via a continuous configuration-interaction approach the authors proved that a state with the translational symmetry can have energy lower than the symmetry breaking solution of the GPE when N is finite. In the regime of the quantum phase transition, the particle correlation becomes much stronger and the condensate becomes fragmented [7]. However, the fragmented condensate tends to approach a single condensate under a symmetry-breaking perturbation [10]. When the perturbation is sufficiently large, the ground state begins to localize by superposition of the quasi-degenerate states [11]. In [13], the author discussed the motion modes in detail and found the low energy spectrum consists of oscillation bands.

Table 1. Eigenenergies E_n with different $(k_{\max}, K_{\max})$.

n	(3, 60)	(4, 60)	(4, 70)	(5, 70)
1	−41.007	−41.067	−41.101	−41.113
9	−35.793	−35.843	−35.880	−35.891
10	−35.650	−35.698	−35.750	−35.762

In this work, we are interested in the stability of the yrast states, each of which is the lowest state of a given total angular momentum, in the regime of quantum phase transition. The ground state and the yrast states of finite angular momenta have been calculated by diagonalizing the many-body Hamiltonian with the single-particle angular momenta up to 4. As expected, the yrast states have spatial translational symmetry. In [10], the distribution of the yrast states in the ground state under a symmetry-breaking perturbation was studied. Similarly, we expand the mean-field soliton wavefunction in the space spanned by the quasi-degenerate yrast states to show that the emergence of the bright soliton state is attributed to the accumulation of yrast states of different angular momenta, which helps to have a better understanding for the nature of the solution of the GPE. We also investigate the influence of a symmetry-breaking perturbation introduced by a ring deformation. Differing from [10, 11], we focus on the mixing dynamics of the quasi-degenerate yrast states. It would be interesting to realize experimentally the coherent oscillation of huge matter predicted in the present paper.

2. Structural transition

We consider a system of N identical bosons confined on a ring. The bosons have mass m and attractive contact-potential interaction. Let R be the ring radius and $\hbar^2/(2mR^2)$ be the unit of energy. The Hamiltonian of the system reads

$$H = -\sum_i \frac{\partial^2}{\partial\theta_i^2} + \frac{U}{2}\sum_{i\neq j}\delta(\theta_i - \theta_j), \tag{1}$$

where θ_i is the azimuthal angle of the ith boson and $U(<0)$ denotes the interaction strength. As shown in [7, 8], the coupling is described by a single dimensionless parameter

$$\gamma \equiv -\frac{UN}{2\pi}. \tag{2}$$

Let $\phi_k = \mathrm{e}^{\mathrm{i}k\theta}/\sqrt{2\pi}$ be the single-particle state, where a cutoff of k, $|k| \leqslant k_{\max}$ is set. Then the normalized basis in the Fock space can be denoted as $|\alpha\rangle \equiv |n_{-k_{\max}}, \ldots, n_{k_{\max}}\rangle$, where $\sum_k n_k = N$, and $\sum_k n_k k = L$ is the total angular momentum. Facilitated by the fractional parentage coefficients [14], the matrix elements of H can be calculated conveniently. Then H is diagonalized in the space spanned by $|\alpha\rangle$, and the low-lying states are worked out.

To make the calculation more efficient, we have limited the kinetic energy of $|\alpha\rangle$, $K_\alpha = \sum_k n_k k^2$, not to exceed a maximum value, i.e., $K_\alpha \leqslant K_{\max}$. Once L, $k_{\max}$ and $K_{\max}$ are set, the basis is then determined, and the eigenenergies $E_n (n \geqslant 1)$ can be calculated. Table 1 shows the values of E_1, E_9 and E_{10} with different $(k_{\max}, K_{\max})$, where $N = 100$, $L = 0$ and $\gamma = 0.7$ are assumed. From table 1, (4, 70) is a reasonable choice of $(k_{\max}, K_{\max})$ and will be used in the latter part of this paper.

A pair of particles excited to $\phi_{\pm 1}$ is called a basic pair where both particles rotate in p-wave but in reverse directions. It was found in [13] that this type of excitation is an elementary mode for the bosons in a ring with repulsive interaction. The role of these basic pairs in

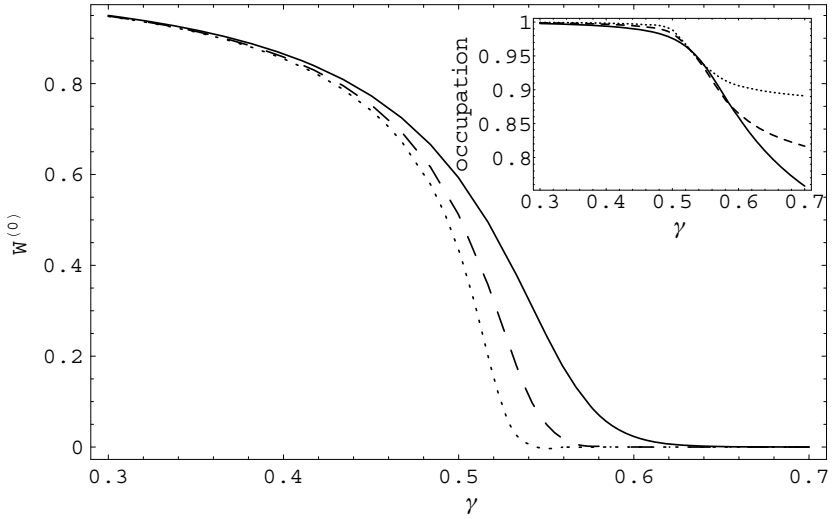

Figure 1. The weight of $|P^{(0)}\rangle$ in the ground state with respect to γ. Inset: occupation of ϕ_0 in the ground state. The solid, dashed and dotted lines correspond to $N = 50$, 100 and 200.

Table 2. The three most important components of the ground state together with their weights $W^{(j)}$.

γ	First	Second	Third
0.40	$\|P^{(0)}\rangle$, 0.859	$\|P^{(1)}\rangle$, 0.119	$\|P^{(2)}\rangle$, 0.016
0.45	$\|P^{(0)}\rangle$, 0.754	$\|P^{(1)}\rangle$, 0.186	$\|P^{(2)}\rangle$, 0.043
0.50	$\|P^{(0)}\rangle$, 0.511	$\|P^{(1)}\rangle$, 0.267	$\|P^{(2)}\rangle$, 0.125
0.55	$\|P^{(3)}\rangle$, 0.167	$\|P^{(4)}\rangle$, 0.155	$\|P^{(2)}\rangle$, 0.147
0.60	$\|P^{(7)}\rangle$, 0.115	$\|P^{(8)}\rangle$, 0.106	$\|P^{(6)}\rangle$, 0.104

our system with attractive interaction will be clarified. We study first the ground state with total angular momentum $L = 0$. The $|\alpha\rangle$ that contains j basic pairs with the other $N - 2j$ particles remaining in ϕ_0 (i.e., not excited), is denoted as $|P^{(j)}\rangle$. In particular, $|P^{(0)}\rangle$ denotes the state without any excitation (all particles are in ϕ_0). It turns out that the ground state with a positive γ (attractive interaction), just as in [13], is dominated by the basic pairs and the wavefunction is a superposition of $|P^{(j)}\rangle$ states, $|G\rangle \sim \sum_j a_j |P^{(j)}\rangle$. This is shown in table 2 where $N = 100$ is assumed and the weights ($W^{(j)} = |a_j|^2$) of the three most important components are given. Disregarding what γ is, all the important components belong to the subspace spanned by $|P^{(j)}\rangle$ without exception. It implies that the excitation of particles to higher partial wave is not important. $W^{(j)}$ changes sharply against γ. When γ is small, $|P^{(0)}\rangle$ is dominant. Accordingly, the particles have high probability to distribute uniformly inside the ring. When γ increases, $W^{(0)}$ reduces as shown in the second column of table 2. When γ is lying between 0.5 and 0.6, $W^{(0)}$ decreases rapidly. Accordingly, the ground state undergoes a great change in structure as discussed in [7, 8]. In the framework of the MFT, the change is a quantum phase transition in which the uniform distribution is replaced by the bright soliton solution. However, by the direct diagonalization method for a finite number of particles, the change is rapid but continuous. The dramatic change of $W^{(0)}$ against γ is plotted in figure 1, where the steep decline is remarkable. It is noted that the steepness depends on N. When N

increases, the decline becomes steeper and its location is closer to $\gamma = 1/2$. One expects that, as $N \to \infty$, the decline would suddenly take place exactly at the theoretical value $1/2$ predicted by the MFT [7, 8], and the associated change of the structure would become a true phase transition. The inset of figure 1 shows the occupation of ϕ_0 in the ground state. Along with the steep decline of $W^{(0)}$, the occupation of ϕ_0 also decreases from unity. This implies that higher single-particle states are macroscopically populated and the condensate becomes fragmented.

When γ is small, the particle interaction is weak, so the kinetic energy dominates the total energy. In this case the ground state would do its best to lower the kinetic energy, this leads to the domination of $|P^{(0)}\rangle$ and accordingly a uniform particle distribution. When γ increases, the relative importance of interaction energy increases as well. Once the interaction energy takes over the kinetic energy, the ground state would make another choice, namely, to do its best to lower the interaction energy by a concentration of the particles. This leads to the breakdown of the translational symmetry and the formation of the bright soliton [7, 8]. In quantum-mechanical systems, the realization of the concentration is given by the interference of the partial waves. Since the p-wave is the one with the lowest excitation energy, it is natural that the ground state would be a superposition of the $|P^{(j)}\rangle$ states as shown by the lowest two rows of table 2. In this case the weights of every $|P^{(j)}\rangle$ are quite smoothly distributed in a wide region of j (e.g., the largest three weights are very close to each other as shown in table 2). This implies a strong fluctuation of the basic pairs.

The parameter γ also affects the particle correlation. To study this effect, the two-body density [7, 13] is employed

$$\rho_2(\theta_1, \theta_2) = \int \mathrm{d}\theta_3 \cdots \mathrm{d}\theta_N \Psi^*(\overrightarrow{\theta})\Psi(\overrightarrow{\theta}), \tag{3}$$

where $\Psi(\overrightarrow{\theta})$ is the wavefunction of the state under consideration, with $\overrightarrow{\theta} = (\theta_1, \ldots, \theta_N)$. Using the fractional parentage coefficients [14], ρ_2 can be calculated in the coordinate space by extracting particles 1 and 2 from $|\alpha\rangle$, i.e.,

$$|\alpha\rangle = \sum_k \sqrt{n_k(n_k-1)/N(N-1)}\phi_k(1)\phi_k(2)|\alpha_k\rangle + \sum_{k_a \neq k_b} \sqrt{n_{k_a} n_{k_b}/N(N-1)}\phi_{k_a}(1)\phi_{k_b}(2)|\alpha_{k_a k_b}\rangle \tag{4}$$

where $|\alpha_k\rangle$ is different from $|\alpha\rangle$ by replacing n_k with $n_k - 2$, $|\alpha_{k_a k_b}\rangle$ is different from $|\alpha\rangle$ by replacing n_{k_a} and n_{k_b} with $n_{k_a} - 1$ and $n_{k_b} - 1$, respectively. Figure 2 presents ρ_2 as a function of θ_2 for the ground state, with $\theta_1 = 0$ given. The results are consistent with a similar discussion in [7]. The particle correlation is very weak when γ is below the critical point, as shown in figure 2(a). However, they become much stronger once γ exceeds the critical point, as shown in figure 2(b), where the dotted curve implies a very strong clustering, namely, all the particles are close to each other.

3. Yrast states

It is recalled that the condensate wavefunction $\psi_0(\theta)$ describing the ground state of the system within the MFT obeys the one-dimensional GPE

$$\left(-\frac{\partial^2}{\partial\theta^2} - 2\pi\gamma|\psi_0|^2\right)\psi_0 = \mu\psi_0, \tag{5}$$

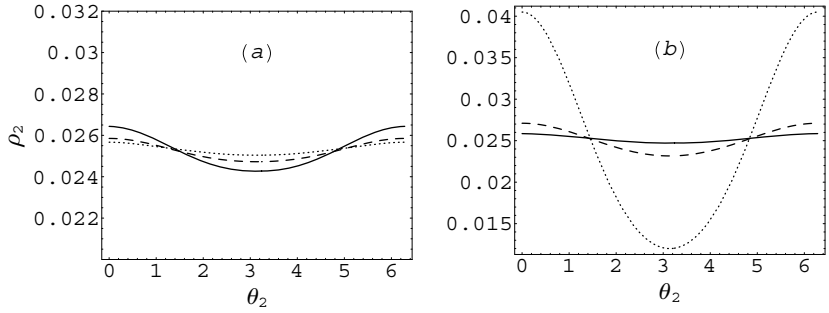

Figure 2. ρ_2 as a function of θ_2 for the ground state with $\theta_1 = 0$ given. (a) $\gamma = 0.4$ is given. The solid, dashed and dotted lines correspond to $N = 50$, 100 and 200. (b) $N = 100$ is given. The solid, dashed and dotted lines correspond to $\gamma = 0.4$, 0.5 and 0.6.

Table 3. The eigenenergies of the ground states obtained by direct diagonalization (the second row) and the MFT (the third row) with different values of γ (the first row) as $N = 100$ is given.

	0.3	0.4	0.5	0.6
Diagonalization	−14.936	−19.985	−25.169	−31.790
MFT	−15.000	−20.000	−25.000	−31.753

where μ is the chemical potential. For $\gamma \leqslant 1/2$, ψ_0 is a constant [6], while for $\gamma > 1/2$, there is a bright soliton solution [7]. The transition of ψ_0 and the ground state are obtained by the diagonalization of the Hamiltonian (1).

Table 3 shows the eigenenergies of the ground states obtained by the two methods with different values of γ and with $N = 100$ given. It is clear that the eigenenergies obtained by two methods are almost the same for all γ considered here. The many-body wavefunction of the bright soliton in the coordinate from a constant to a bright soliton at $\gamma_{cr} = 1/2$ indicates a quantum phase transition in the system. In the following, we discuss the relation between the yrast state and the bright soliton state obtained by the MFT representation which reads $\Psi(\overrightarrow{\theta}) = \prod_i \psi_0(\theta_i)$. Since the eigenstates of the Hamiltonian are complete, $\Psi(\overrightarrow{\theta})$ can be expanded as

$$\Psi(\overrightarrow{\theta}) = \sum_{n,L} C_n^L \Psi_n^L, \tag{6}$$

where Ψ_n^L is the nth eigenstate of angular momentum L, and C_n^L is the corresponding composition coefficient. Since the energy of the bright soliton is close to the ground-state energy, the bright soliton should be mainly composed of the yrast states (i.e., Ψ_1^L). In figure 3, numerical results of $\left|C_1^L\right|^2$ for $\gamma = 0.55$, 0.6 and 0.65 are shown (obviously, $\left|C_1^{-L}\right|^2 = \left|C_1^L\right|^2$), where the weights distribute in quite a broad range of L. As γ increases, the distribution becomes even broader, which means the yrast states with finite L play an important role in the bright soliton. This behavior is associated with that the shape of the condensate wavefunction becomes narrower and sharper as γ increases, as shown in the inset of figure 3. The inclusion of different yrast states counts for the non-uniform spatial wavefunction.

Let $E(L)$ be the eigenenergy of the yrast state of L. To compare with the exact ground state, we plot $(E(L) - E(0))/|E(0)|$ with respect to L with different γ in figure 4. It is clear that the yrast state of $L = 0$ is the exact ground state. The energy increases linearly

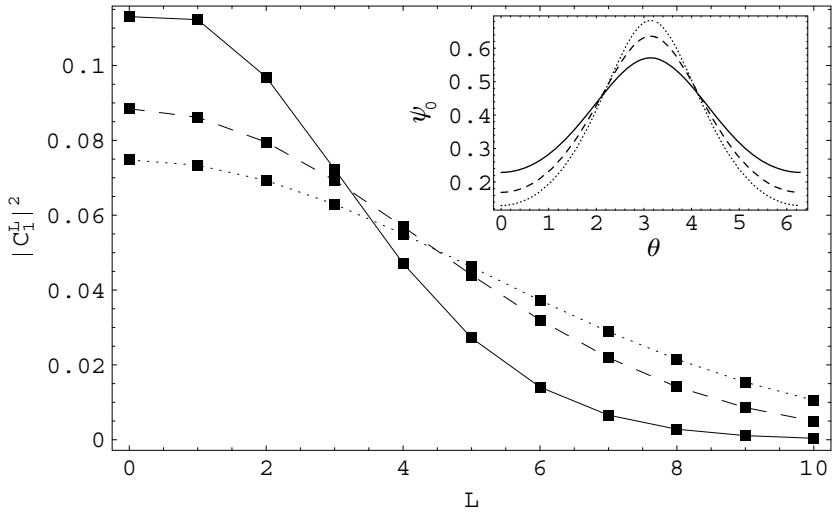

Figure 3. $|C_1^L|^2$ of the yrast states with $L = 0$ to 10 in the bright soliton with $\gamma = 0.55$ (solid), 0.6 (dashed) and 0.65(dotted). The inset shows the condensate wavefunctions of the bright solitons with the corresponding values of γ.

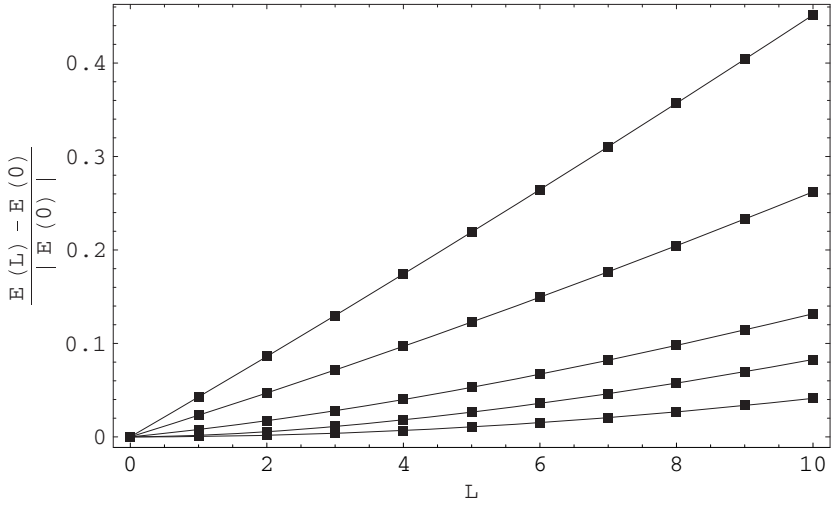

Figure 4. $(E(L) - E(0))/|E(0)|$ of the yrast states with $L = 0$ to 10. Lines from top to bottom correspond to $\gamma = 0.3$, 0.4, 0.5, 0.55 and 0.65, $N = 100$ is given.

when interaction strength is weak. The energy increase becomes nonlinear and much slower for larger γ. When γ is above the critical point, the eigenenergies of the first several yrast states are almost the same, as shown in the two lowest lines in figure 4. It is consistent with that the ground state is quasi-degenerate in the strong-interaction phase [10]. The energy gap between the ground and first excited states tends to disappear as particle interaction increases.

4. Cluster states

Consider a ring having a small geometric deformation that breaks the spatial translational symmetry, e.g., an elliptic ring whose curvature is

$$\kappa(\theta) = \frac{\sqrt{1+\eta}}{(1+\eta\sin^2\theta)^{3/2}}, \tag{7}$$

where θ is the azimuthal angle and $\eta > 0$ is a small quantity. Its effect on the condensate can be estimated approximately by the degenerate perturbation theory. The perturbative Hamiltonian due to the deformation reads [15]

$$H' = -\frac{1}{4}\sum_i(\kappa^2(\theta_i) - 1). \tag{8}$$

The Hamiltonian is invariant in two transformations: (1) $\theta \to \theta + \pi$; (2) $\theta \to -\theta$. They are referred to as I-parity and P-parity transformations. Therefore, the state space is divided into four invariant subspaces according to the (I, P) parity of the states, where $(I, P) = (\pm, \pm)$. The subspace of yrast states can be spanned by the parity conserved bases

$$f_0^+ = \Psi_1^0, \qquad f_L^\pm = \tfrac{1}{\sqrt{2}}\left(\Psi_1^L \pm \Psi_1^{-L}\right), \tag{9}$$

where $L \geqslant 1$ is assumed. The states $f_L^\pm$ have parities $((-1)^L, \pm)$. The state f_0^- does not exist.

As discussed above, the first several yrast states are quasi-degenerate when $\gamma > \gamma_{cr}$. The proper zero-order wavefunctions of parity (I, P) are linear combinations of f-bases of the same parity

$$\begin{aligned} \chi^{++} &= \sum_{n=0}\beta_{2n}^{++} f_{2n}^+, & \chi^{+-} &= \sum_{n=1}\beta_{2n}^{+-} f_{2n}^-, \\ \chi^{-+} &= \sum_{n=0}\beta_{2n+1}^{-+} f_{2n+1}^+, & \chi^{--} &= \sum_{n=0}\beta_{2n+1}^{--} f_{2n+1}^-, \end{aligned} \tag{10}$$

where $\beta_L^{I,P}$ are the composition coefficients. The nonzero matrix elements of H' are $s = \langle f_1^+|H'|f_1^+\rangle = -\langle f_1^-|H'|f_1^-\rangle$, $u_{L,L+2l} = \langle f_L^+|H'|f_{L+2l}^+\rangle = \langle f_L^-|H'|f_{L+2l}^-\rangle$ (l is a positive integer), and their complex conjugates. These matrix elements can be calculated when the yrast states are known. For a small deformation, to the first order of η, only elements of $l = 1$ remain. Then $u_{L,L+2}$ and s are proportional to η.

For simplicity, here we only consider the lowest nine yrast states with $|L| \leqslant 4$. The parity conserved bases for this subspace are f_0^+ and $f_L^\pm$ with $L = 1$–4. The main finding will be still valid if more yrast states are included. The subspaces $(+,+)$, $(+,-)$, $(-,+)$ and $(-,-)$ have base sets $\{f_0^+, f_2^+, f_4^+\}$, $\{f_2^-, f_4^-\}$, $\{f_1^+, f_3^+\}$ and $\{f_1^-, f_3^-\}$, respectively. To the first order of η, the energy corrections are

$$\begin{aligned} E_{1,2}^{++} &= \mp\sqrt{|u_{02}|^2 + |u_{24}|^2}, & E_3^{++} &= 0; \\ E_{1,2}^{+-} &= \mp|u_{24}|; \\ E_{1,2}^{-+} &= \tfrac{1}{2}\left(s \mp \sqrt{4|u_{13}|^2 + s^2}\right); \\ E_{1,2}^{--} &= \tfrac{1}{2}\left(-s \mp \sqrt{4|u_{13}|^2 + s^2}\right). \end{aligned} \tag{11}$$

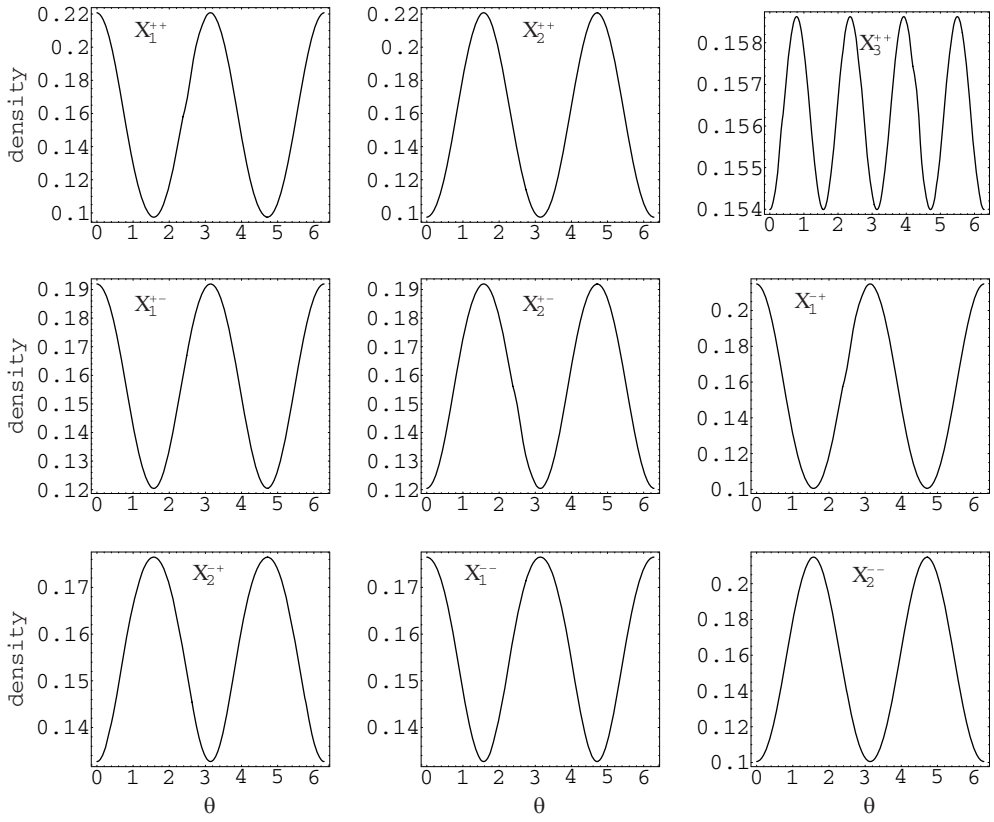

Figure 5. The single-particle densities of the proper zero-order wavefunctions under the perturbative deformation of the ring, $\gamma = 0.65$, $N = 100$.

The corresponding wavefunctions are

$$\chi_{1,2}^{++} = \frac{1}{\sqrt{2}}\left(\frac{|u_{02}|}{|E_1^{++}|}f_0^+ \mp f_2^+ + \frac{|u_{24}|}{|E_1^{++}|}f_4^+\right), \qquad \chi_3^{++} = -\frac{|u_{24}|}{|E_1^{++}|}f_0^+ + \frac{|u_{02}|}{|E_1^{++}|}f_4^+;$$

$$\chi_{1,2}^{+-} = \frac{1}{\sqrt{2}}(f_2^- \pm f_4^-);$$

$$\chi_{1,2}^{-+} = \frac{E_{1,2}^{-+}}{\sqrt{(E_{1,2}^{-+})^2 + 4|u_{13}|^2}}f_1^+ + \frac{2|u_{13}|}{\sqrt{(E_{1,2}^{-+})^2 + 4|u_{13}|^2}}f_3^+; \tag{12}$$

$$\chi_{1,2}^{--} = \frac{E_{1,2}^{--}}{\sqrt{(E_{1,2}^{--})^2 + 4|u_{13}|^2}}f_1^- + \frac{2|u_{13}|}{\sqrt{(E_{1,2}^{--})^2 + 4|u_{13}|^2}}f_3^-.$$

The notation should be self-understandable.

Numerically, it is not difficult to include the higher order corrections to the energies. For instance, the condensate of $N = 100$, with $\gamma = 0.65$ in a deformed ring with $\eta = 0.21$ is calculated. The reduced single-particle density of $\chi_n^{I,P}$ is plotted in figure 5, which clearly shows the cluster structure with breaking spatial symmetry. Figure 5 shows that the particles tend to concentrate at the ends of the two orthogonal axes except for the case

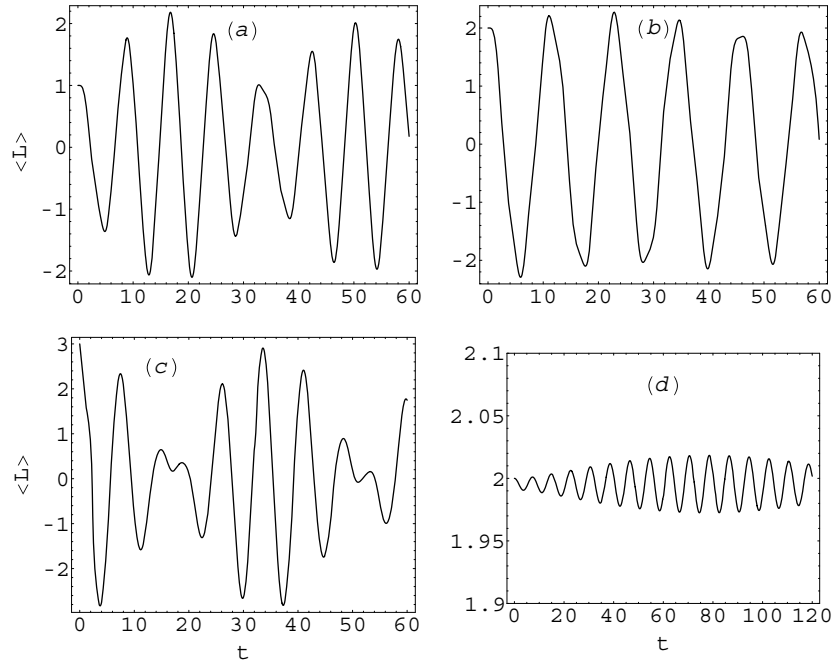

Figure 6. Time evolution of the average angular momentum under a perturbative deformation of the ring. Parts (*a*)–(*c*) correspond to different initial states from Ψ_1^1 to Ψ_1^3 with $\gamma = 0.65$. Part (*d*) corresponds to the initial state Ψ_1^2 with $\gamma = 0.45$. t is in unit of $2mR^2/\hbar$, $N = 100$.

of χ_3^{++}. The two-peak cluster of χ_1^{++} is expected to be the stablest state under the geometric perturbation.

With the proper zero-order wavefunctions, one is able to calculate the probabilities of transitions between different yrast states after the perturbative deformation is turned on. Assume that the condensate is in $\Psi_1^{L_0}$ at time $t = 0$, and the perturbative deformation is turned on suddenly. Then the probability of the condensate being in Ψ_1^L at time $t > 0$ takes the form

$$\mathcal{P}_{L,L_0}(t) = \left| \sum_{P,n} \left(A_{L_0}^{I,P,n}\right)^* A_L^{I,P,n} \exp\left(-\mathrm{i}E_n^{I,P}t\right) \right|^2, \tag{13}$$

where $I = (-1)^{L_0}$, $A_L^{I,P,n}$ are the composition coefficients of Ψ_1^L in $\chi_n^{I,P}$, which are given by inserting (9) into (10) and making use of (12), $E_n^{I,P}$ are given by (11) and t is in unit of $2mR^2/\hbar$. The angular momentum L should have the same I-parity as L_0, or the transition is forbidden. Furthermore, the average angular momentum of the condensate at time t can be expressed as

$$\langle \mathcal{L}(t; L_0) \rangle = \sum_L L\mathcal{P}_{L,L_0}(t). \tag{14}$$

It is obvious that $\langle \mathcal{L}(t; -L_0) \rangle = -\langle \mathcal{L}(t; L_0) \rangle$ and $\langle \mathcal{L}(t; 0) \rangle = 0$. For $L_0 \neq 0$, figures 6(*a*)–(*c*) show the time evolution of $\langle \mathcal{L}(t; L_0) \rangle$ with L_0 arranged from 1 to 3. It is remarkable that $\langle \mathcal{L}(t; L_0) \rangle$ undergoes an irregular oscillation with a large amplitude. This is a remarkable physical effect of the quantum phase transition on the condensate. As a result of the quasi-degeneration of the yrast states, they mix together strongly under even small perturbation,

which leads to the strong fluctuation of $\langle \mathcal{L}(t; L_0)\rangle$. For $\gamma < \gamma_{cr}$, the energy differences between different yrast states are relatively large, the probabilities of transitions between them are consequently very small. As shown in figure 6(*d*), for $\gamma = 0.45$, the fluctuation is about two orders smaller than that of $\gamma = 0.65$.

In principle, low lying states Ψ_n^L with $n > 1$ other than the yrast states might be mixed up under a larger perturbation. This enables the transition from the quasi-degenerate ground band to low excited bands and leads to a more complex mixing dynamics.

To observe the angular momentum oscillation, one should first prepare a vortex state with $L \neq 0$ in a symmetric ring. It would be easier to realize the vortex state in the non-critical regime ($\gamma < \gamma_{cr}$) where the yrast states are not degenerate. Then the coupling is tuned to a value larger than γ_{cr} and modify the trap to a elliptic ring.

5. Conclusion

In summary, we have studied the *N*-boson system confined on the ring with attractive interaction between the particles. By diagonalizing the many-body Hamiltonian, we investigated the ground state and the yrast states, with interest in the quantum phase transition driven by the coupling parameter γ. The probability of all atoms remaining in zero momentum drops dramatically as γ exceeds the critical point, which signals the quantum phase transition. The two-body correlation shows that the particles have large tendency to concentrate in space if γ is larger than the critical value. However, the yrast states still have the spatial symmetry. The symmetry breaking phenomenon, i.e., the clustering in the strong-interaction phase is attributed to the superposition of the yrast states of small L that are quasi-degenerate with the exact ground state. This can be seen more clearly by introducing the perturbation of the geometric deformation that splits the quasi-degenerate yrast states. The reduced single-particle densities exhibit cluster structures where the spatial symmetry is explicitly broken. Due to the perturbation, the yrast states with given angular momenta will mix together in the evolution, and the average angular momentum of the condensate will oscillate strongly. The remarkable mixing dynamics due to the quantum phase transition may be observed in the future experiments since the mixing is strong when the yrast states become quasi-degenerate.

Acknowledgments

The authors are grateful to Professor C G Bao for suggesting this topic and many helpful discussions. The support from the NSFC under the grants 10574163 and 90306016, and from National Basic Research Program of China (2007CB935500) are appreciated.

References

[1] Görlitz A *et al* 2001 *Phys. Rev. Lett.* **87** 130402
[2] Inouye S, Andrews M R, Stenger J, Miesner H J, Stamper-Kurn D M and Ketterle W 1998 *Nature (London)* **392** 151
[3] Khaykovich L, Schreck F, Ferrari G, Bourdel T, Cubizolles J, Carr L D, Castin Y and Salomon C 2002 *Science* **296** 1290
[4] Strecker K E, Partridge G B, Truscott A G and Hulet R G 2002 *Nature (London)* **417** 150
[5] Carr L D, Clark C W and Reinhardt W P 2000 *Phys. Rev.* A **62** 063610
[6] Carr L D, Clark C W and Reinhardt W P 2000 *Phys. Rev.* A **62** 063611
[7] Kanamoto R, Saito H and Ueda M 2003 *Phys. Rev.* A **67** 013608
[8] Kavoulakis G M 2003 *Phys. Rev.* A **67** 011601

[9] Alon O E, Streltsov A I, Sakmann K and Cederbaum L S 2004 *Europhys. Lett.* **67** 8
[10] Kanamoto R, Saito H and Ueda M 2005 *Phys. Rev. Lett.* **94** 090404
[11] Kanamoto R, Saito H and Ueda M 2006 *Phys. Rev.* A **73** 033611
[12] Parola A, Salasnich L, Rota R and Reatto L 2005 *Phys. Rev.* A **72** 063612
[13] Bao C G 2007 *Phys. Rev.* A **75** 063626
[14] Bacher F and Goudsmit S 1934 *Phys. Rev.* **46** 948
[15] Leboeuf P and Pavloff N 2001 *Phys. Rev.* A **64** 033602